



Title	J/ψ + ψ' - Resonant structure around 1.8GeV/c ² and $\psi(1405)$ in ψ + ψ'
-------	---

$\eta\pi^+\pi^-$ Resonant Structure around 1.8 GeV/ c^2 and $\eta(1405)$ in $J/\psi \rightarrow \omega\eta\pi^+\pi^-$

M. Ablikim,¹ M. N. Achasov,⁵ D. Alberto,⁴¹ Q. An,³⁹ Z. H. An,¹ J. Z. Bai,¹ R. Baldini,¹⁹ Y. Ban,²⁵ J. Becker,² N. Berger,¹ M. Bertani,¹⁹ J. M. Bian,¹ O. Bondarenko,¹⁸ I. Boyko,¹⁷ R. A. Briere,³ V. Bytev,¹⁷ X. Cai,¹ A. C. Calcaterra,¹⁹ G. F. Cao,¹ X. X. Cao,¹ J. F. Chang,¹ G. Chelkov,^{17a} G. Chen,¹ H. S. Chen,¹ J. C. Chen,¹ M. L. Chen,¹ S. J. Chen,²³ Y. Chen,¹ Y. B. Chen,¹ H. P. Cheng,¹³ Y. P. Chu,¹ D. Cronin-Hennessy,³⁸ H. L. Dai,¹ J. P. Dai,¹ D. Dedovich,¹⁷ Z. Y. Deng,¹ I. Denysenko,^{17b} M. Destefanis,⁴¹ Y. Ding,²¹ L. Y. Dong,¹ M. Y. Dong,¹ S. X. Du,⁴⁵ R. R. Fan,¹ J. Fang,¹ S. S. Fang,¹ C. Q. Feng,³⁹ C. D. Fu,¹ J. L. Fu,²³ Y. Gao,³⁵ C. Geng,³⁹ K. Goetzen,⁷ W. X. Gong,¹ M. Greco,⁴¹ S. Grishin,¹⁷ M. H. Gu,¹ Y. T. Gu,⁹ Y. H. Guan,⁶ A. Q. Guo,²⁴ L. B. Guo,²² Y. P. Guo,²⁴ X. Q. Hao,¹ F. A. Harris,³⁷ K. L. He,¹ M. He,¹ Z. Y. He,²⁴ Y. K. Heng,¹ Z. L. Hou,¹ H. M. Hu,¹ J. F. Hu,⁶ T. Hu,¹ B. Huang,¹ G. M. Huang,¹⁴ J. S. Huang,¹¹ X. T. Huang,²⁷ Y. P. Huang,¹ T. Hussain,⁴⁰ C. S. Ji,³⁹ Q. Ji,¹ X. B. Ji,¹ X. L. Ji,¹ L. K. Jia,¹ L. L. Jiang,¹ X. S. Jiang,¹ J. B. Jiao,²⁷ Z. Jiao,¹³ D. P. Jin,¹ S. Jin,¹ F. F. Jing,³⁵ N. Kalantar-Nayestanaki,¹⁸ M. Kavatsyuk,¹⁸ S. Komamiya,³⁴ W. Kuehn,³⁶ J. S. Lange,³⁶ J. K. C. Leung,³³ Cheng Li,³⁹ Cui Li,³⁹ D. M. Li,⁴⁵ F. Li,¹ G. Li,¹ H. B. Li,¹ J. C. Li,¹ K. Li,¹⁰ Lei Li,¹ N. B. Li,²² Q. J. Li,¹ W. D. Li,¹ W. G. Li,¹ X. L. Li,²⁷ X. N. Li,¹ X. Q. Li,²⁴ X. R. Li,¹ Z. B. Li,³¹ H. Liang,³⁹ Y. F. Liang,²⁹ Y. T. Liang,³⁶ X. T. Liao,¹ B. J. Liu,³³ B. J. Liu,³² C. L. Liu,³ C. X. Liu,¹ C. Y. Liu,¹ F. H. Liu,²⁸ Fang Liu,¹ Feng Liu,¹⁴ G. C. Liu,¹ H. Liu,¹ H. B. Liu,⁶ H. H. Liu,¹² H. M. Liu,¹ H. W. Liu,¹ J. P. Liu,⁴³ K. Liu,²⁵ K. Liu,⁶ K. Y. Liu,²¹ Q. Liu,³⁷ S. B. Liu,³⁹ X. Liu,²⁰ X. H. Liu,¹ Y. B. Liu,²⁴ Y. W. Liu,³⁹ Yong Liu,¹ Z. A. Liu,¹ Z. Q. Liu,¹ H. Loehner,¹⁸ G. R. Lu,¹¹ H. J. Lu,¹³ J. G. Lu,¹ Q. W. Lu,²⁸ X. R. Lu,⁶ Y. P. Lu,¹ C. L. Luo,²² M. X. Luo,⁴⁴ T. Luo,¹ X. L. Luo,¹ C. L. Ma,⁶ F. C. Ma,²¹ H. L. Ma,¹ Q. M. Ma,¹ T. Ma,¹ X. Ma,¹ X. Y. Ma,¹ M. Maggiora,⁴¹ Q. A. Malik,⁴⁰ H. Mao,¹ Y. J. Mao,²⁵ Z. P. Mao,¹ J. G. Messchendorp,¹⁸ J. Min,¹ R. E. Mitchell,¹⁶ X. H. Mo,¹ N. Yu. Muchnoi,⁵ Y. Nefedov,¹⁷ I. B. Nikolaev,⁵ Z. Ning,¹ S. L. Olsen,²⁶ Q. Ouyang,¹ S. Pacetti,¹⁹ M. Pelizaeus,³⁷ K. Peters,⁷ J. L. Ping,²² R. G. Ping,¹ R. Poling,³⁸ C. S. J. Pun,³³ M. Qi,²³ S. Qian,¹ C. F. Qiao,⁶ X. S. Qin,¹ J. F. Qiu,¹ K. H. Rashid,⁴⁰ G. Rong,¹ X. D. Ruan,⁹ A. Sarantsev,^{17c} J. Schulze,² M. Shao,³⁹ C. P. Shen,^{37d} X. Y. Shen,¹ H. Y. Sheng,¹ M. R. Shepherd,¹⁶ X. Y. Song,¹ S. Sonoda,³⁴ S. Spataro,⁴¹ B. Spruck,³⁶ D. H. Sun,¹ G. X. Sun,¹ J. F. Sun,¹¹ S. S. Sun,¹ X. D. Sun,¹ Y. J. Sun,³⁹ Y. Z. Sun,¹ Z. J. Sun,¹ Z. T. Sun,³⁹ C. J. Tang,²⁹ X. Tang,¹ H. L. Tian,¹ D. Toth,³⁸ G. S. Varner,³⁷ X. Wan,¹ B. Q. Wang,²⁵ K. Wang,¹ L. L. Wang,⁴ L. S. Wang,¹ M. Wang,²⁷ P. Wang,¹ P. L. Wang,¹ Q. Wang,¹ S. G. Wang,²⁵ X. L. Wang,³⁹ Y. D. Wang,³⁹ Y. F. Wang,¹ Y. Q. Wang,²⁷ Z. Wang,¹ Z. G. Wang,¹ Z. Y. Wang,¹ D. H. Wei,⁸ Q. G. Wen,³⁹ S. P. Wen,¹ U. Wiedner,² L. H. Wu,¹ N. Wu,¹ W. Wu,²¹ Z. Wu,¹ Z. J. Xiao,²² Y. G. Xie,¹ G. F. Xu,¹ G. M. Xu,²⁵ H. Xu,¹ Q. J. Xu,¹⁰ X. P. Xu,³⁰ Y. Xu,²⁴ Z. R. Xu,³⁹ Z. Z. Xu,³⁹ Z. Xue,¹ L. Yan,³⁹ W. B. Yan,³⁹ Y. H. Yan,¹⁵ H. X. Yang,¹ M. Yang,¹ T. Yang,⁹ Y. Yang,¹⁴ Y. X. Yang,⁸ M. Ye,¹ M. H. Ye,⁴ B. X. Yu,¹ C. X. Yu,²⁴ L. Yu,¹⁴ S. P. Yu Yu,²⁷ C. Z. Yuan,¹ W. L. Yuan,²² Y. Yuan,¹ A. A. Zafar,⁴⁰ A. Zallo,¹⁹ Y. Zeng,¹⁵ B. X. Zhang,¹ B. Y. Zhang,¹ C. C. Zhang,¹ D. H. Zhang,¹ H. H. Zhang,³¹ H. Y. Zhang,¹ J. Zhang,²² J. W. Zhang,¹ J. Y. Zhang,¹ J. Z. Zhang,¹ L. Zhang,²³ S. H. Zhang,¹ T. R. Zhang,²² X. J. Zhang,¹ X. Y. Zhang,²⁷ Y. Zhang,¹ Y. H. Zhang,¹ Z. P. Zhang,³⁹ Z. Y. Zhang,⁴³ G. Zhao,¹ H. S. Zhao,¹ Jiawei Zhao,³⁹ Jingwei Zhao,¹ Lei Zhao,³⁹ Ling Zhao,¹ M. G. Zhao,²⁴ Q. Zhao,¹ S. J. Zhao,⁴⁵ T. C. Zhao,⁴² X. H. Zhao,²³ Y. B. Zhao,¹ Z. G. Zhao,³⁹ Z. L. Zhao,⁹ A. Zhemchugov,^{17a} B. Zheng,¹ J. P. Zheng,¹ Y. H. Zheng,⁶ Z. P. Zheng,¹ B. Zhong,¹ J. Zhong,² L. Zhong,³⁵ L. Zhou,¹ X. K. Zhou,⁶ X. R. Zhou,³⁹ C. Zhu,¹ K. Zhu,¹ K. J. Zhu,¹ S. H. Zhu,¹ X. L. Zhu,³⁵ X. W. Zhu,¹ Y. S. Zhu,¹ Z. A. Zhu,¹ J. Zhuang,¹ B. S. Zou,¹ J. H. Zou,¹ and J. X. Zuo¹

(BESIII Collaboration)

¹Institute of High Energy Physics, Beijing 100049, China²Bochum Ruhr-University, 44780 Bochum, Germany³Carnegie Mellon University, Pittsburgh, Pennsylvania 15213, USA⁴China Center of Advanced Science Technology, Beijing 100190, China⁵G.I. Budker Institute of Nuclear Physics SB RAS (BINP), Novosibirsk 630090, Russia⁶Graduate University of Chinese Academy of Sciences, Beijing 100049, China⁷GSI Helmholtzcentre for Heavy Ion Research GmbH, D-64291 Darmstadt, Germany⁸Guangxi Normal University, Guilin 541004, China⁹Guangxi University, Nanning 530004, China¹⁰Hangzhou Normal University, XueLin Jie 16, Xiasha Higher Education Zone, Hangzhou 310036, China¹¹Henan Normal University, Xinxiang 453007, China¹²Henan University of Science and Technology

- ¹³Huangshan College, Huangshan 245000, China
¹⁴Huazhong Normal University, Wuhan 430079, China
¹⁵Hunan University, Changsha 410082, China
¹⁶Indiana University, Bloomington, Indiana 47405, USA
¹⁷Joint Institute for Nuclear Research, 141980 Dubna, Russia
^{17a}also at the Moscow Institute of Physics Technology, Moscow, Russia
^{17b}on leave from the Bogolyubov Institute for Theoretical Physics, Kiev, Ukraine
^{17c}also at the PNPI, Gatchina, Russia
¹⁸KVI/University of Groningen, 9747 AA Groningen, The Netherlands
¹⁹Laboratori Nazionali di Frascati - INFN, 00044 Frascati, Italy
²⁰Lanzhou University, Lanzhou 730000, China
²¹Liaoning University, Shenyang 110036, China
²²Nanjing Normal University, Nanjing 210046, China
²³Nanjing University, Nanjing 210093, China
²⁴Nankai University, Tianjin 300071, China
²⁵Peking University, Beijing 100871, China
²⁶Seoul National University, Seoul, 151-747 Korea
²⁷Shandong University, Jinan 250100, China
²⁸Shanxi University, Taiyuan 030006, China
²⁹Sichuan University, Chengdu 610064, China
³⁰Soochow University, Suzhou 215006, China
³¹Sun Yat-Sen University, Guangzhou 510275, China
³²The Chinese University of Hong Kong, Shatin, N. T. Hong Kong
³³The University of Hong Kong, Pokfulam, Hong Kong
³⁴The University of Tokyo, Tokyo 113-0033 Japan
³⁵Tsinghua University, Beijing 100084, China
³⁶Universitaet Giessen 35392 Giessen, Germany
³⁷University of Hawaii, Honolulu, Hawaii 96822, USA
^{37d}now at Nagoya University, Nagoya, Japan
³⁸University of Minnesota, Minneapolis, Minnesota 55455, USA
³⁹University of Science Technology of China, Hefei 230026, China
⁴⁰University of the Punjab, Lahore-54590, Pakistan
⁴¹University of Turin INFN, Turin, Italy
⁴²University of Washington, Seattle, Washington 98195, USA
⁴³Wuhan University, Wuhan 430072, China
⁴⁴Zhejiang University, Hangzhou 310027, China
⁴⁵Zhengzhou University, Zhengzhou 450001, China

(Received 9 July 2011; published 25 October 2011)

We present results of a study of the decay $J/\psi \rightarrow \omega \eta \pi^+ \pi^-$ using a sample of $(225.2 \pm 2.8) \times 10^6$ J/ψ events collected by the BESIII detector, and report the observation of a new process $J/\psi \rightarrow \omega X(1870)$ with a statistical significance of 7.2σ , in which $X(1870)$ decays to $a_0^\pm(980)\pi^\mp$. Fitting to $\eta \pi^+ \pi^-$ mass spectrum yields a mass $M = 1877.3 \pm 6.3(\text{stat})_{-7.4}^{+3.4}(\text{syst})$ MeV/ c^2 , a width $\Gamma = 57 \pm 12(\text{stat})_{-4}^{+19}(\text{syst})$ MeV/ c^2 , and a product branching fraction $\mathcal{B}(J/\psi \rightarrow \omega X) \times \mathcal{B}(X \rightarrow a_0^\pm(980)\pi^\mp) \times \mathcal{B}(a_0^\pm(980) \rightarrow \eta \pi^\pm) = [1.50 \pm 0.26(\text{stat})_{-0.36}^{+0.72}(\text{syst})] \times 10^{-4}$. Signals for $J/\psi \rightarrow \omega f_1(1285)$ and $J/\psi \rightarrow \omega \eta(1405)$ are also clearly observed and measured.

DOI: 10.1103/PhysRevLett.107.182001

PACS numbers: 13.85.Hd, 13.25.Ft, 25.75.Gz

The resonance known as the $X(1835)$, was first observed in the $\eta' \pi^+ \pi^-$ mass spectrum of $J/\psi \rightarrow \gamma \eta' \pi^+ \pi^-$ by BESII [1] and subsequently confirmed with a much higher signal significance by BESIII [2]. Several theoretical speculations have been proposed to interpret the nature of $X(1835)$, including the $p\bar{p}$ bound state [3–5] that was first observed near the same mass in $J/\psi \rightarrow \gamma p\bar{p}$ at BESII [6] and confirmed by BESIII and CLEO [7], a second radial excitation of the η' [8], and a pseudoscalar glueball [9–11]. In the lower mass region of the $\eta \pi^+ \pi^-$ mass spectrum,

around 1.4 GeV/ c^2 , extensive studies [12–14] have established the existence of the $\eta(1405)$, which has also been suggested as a candidate for a pseudoscalar glueball [15]. Experimentally, the study of the production mechanism of the $X(1835)$ and $\eta(1405)$, e.g., searches for them in $\eta \pi^+ \pi^-$ final states with other accompanying particles (ω , ϕ , etc.), are useful for clarifying their nature. In particular, the measurements of the production widths of these two states in hadronic decays of the J/ψ and a comparison with corresponding measurements in J/ψ

radiative decays would provide important information about the glueball possibility [16].

In this Letter, we present the results of a study of $J/\psi \rightarrow \omega \eta \pi^+ \pi^-$. A structure around 1.8–1.9 GeV/ c^2 in the $\eta \pi^+ \pi^-$ mass spectrum is observed. This analysis is based on a sample of $(225.2 \pm 2.8) \times 10^6$ J/ψ events [17] accumulated in the Beijing Spectrometer (BESIII) [18] operating at the Beijing Electron-Positron Collider (BEPCII) [19] at the Beijing Institute of High Energy Physics.

BEPCII is a double-ring e^+e^- collider designed to provide e^+e^- beams with a peak luminosity of 10^{33} cm $^{-2}$ s $^{-1}$ at a beam current of 0.93 A. The cylindrical core of the BESIII detector consists of a helium-based main drift chamber (MDC), a plastic scintillator time-of-flight (TOF) system, and a CsI(Tl) electromagnetic calorimeter (EMC) that are all enclosed in a superconducting solenoidal magnet providing a 1.0 T magnetic field. The solenoid is supported by an octagonal flux-return yoke with resistive plate counter muon identifier modules interleaved with steel. The acceptance of charged particles and photons is 93% of 4π sr, and the charged-particle momentum and photon energy resolutions at 1 GeV are 0.5% and 2.5%, respectively. The BESIII detector is modeled with a Monte Carlo (MC) simulation based on GEANT4 [20,21].

Charged tracks in the BESIII detector are reconstructed using track-induced signals in the MDC. To optimize the momentum measurement, we select tracks in the polar angle range $|\cos\theta| < 0.93$ and require that they pass within ± 20 cm from the interaction point in the beam direction and within ± 2 cm of the beam line in the plane perpendicular to the beam. Four tracks with net charge zero are required and all tracks are assumed to be pions.

Electromagnetic showers are reconstructed from clusters of energy deposits in the EMC. The energy deposited in nearby TOF counters is included to improve the reconstruction efficiency and energy resolution. Showers identified as photon candidates must satisfy fiducial and shower-quality requirements, i.e., the showers in the barrel region ($|\cos\theta| < 0.8$) must have a minimum energy of 25 MeV, while those from the end caps ($0.86 < |\cos\theta| < 0.92$) must have at least 50 MeV. The showers in the angular range between the barrel and end cap are poorly reconstructed and excluded from the analysis. To suppress showers from charged particles, a photon must be separated by at least 10° from the nearest charged track. The EMC cluster timing requirements are used to suppress electronic noise and energy deposits unrelated to the event.

In the reconstruction of $J/\psi \rightarrow \omega \eta \pi^+ \pi^-$, the ω is reconstructed via its $\pi^+ \pi^- \pi^0$ mode, and the η and π^0 are reconstructed from $\gamma\gamma$ pairs. The vertex of all final state particles must be consistent with the measured beam interaction point. The sum of the four-momenta of all particles is constrained to the known J/ψ mass and the initial e^+e^- three-momentum in the lab frame. The vertex and four-momentum kinematic fits are required to satisfy

the quality requirements $\chi^2_{\text{V}}/\text{d.o.f.} < 100/3$ and $\chi^2_{4C}/\text{d.o.f.} < 50/4$, respectively. Further selections are based on the four-momenta from the kinematic fit. Photon pairs with an invariant mass satisfying $M_{\gamma\gamma} \in (524, 572)$ MeV/ c^2 or $(122, 148)$ MeV/ c^2 are identified as η or π^0 candidates. The $\eta \pi^0 4\pi$ combination with minimum χ^2_{4C} is selected in the cases where more than one candidate satisfies the above requirements in an event. If there is more than one four-photon combination in the mass range of the η and π^0 , the assignment with the lowest value of $\chi_{\eta\pi^0} = \sqrt{P_\eta^2 + P_{\pi^0}^2}$ is used, where P_{η/π^0} are the pulls defined as $P_{\eta/\pi^0} = \frac{M_{\gamma\gamma} - m_{\eta/\pi^0}}{\sigma_{\gamma\gamma}}$. Here $\sigma_{\gamma\gamma}$ is the η/π^0 mass resolution determined from data.

After the application of the above requirements, the scatter plot of $M_{\eta(\gamma\gamma)}$ versus $M_{\omega(\pi^+ \pi^- \pi^0)}$ (shown in Fig. 1) shows a clear cluster in the $J/\psi \rightarrow \omega \eta \pi^+ \pi^-$ signal region denoted by the rectangle in the center of the plot. To determine which $\pi^+ \pi^-$ pair originates from the ω , $|M_{\pi^+ \pi^- \pi^0} - m_\omega|$ is minimized among the possible combinations of the selected charged pions, and required to be less than 28 MeV/ c^2 .

With all the selection criteria applied, the mass spectrum of $\eta \pi^+ \pi^-$ is shown in Fig. 2(a). In the lower mass range, in addition to the well-known η' peak, two other structures are observed; these are inferred to be the $f_1(1285)$ and $\eta(1405)$ based on the fit results discussed below. There is an additional structure located around 1.87 GeV/ c^2 that we denote as $X(1870)$. The $\eta \pi^\pm$ mass spectrum for these events, shown in Fig. 2(b), reveals a strong $a_0(980)$ signal. The $\eta \pi^+ \pi^-$ mass spectrum for events where either $M(\eta \pi^+)$ or $M(\eta \pi^-)$ is in a 100 MeV/ c^2 mass window centered on the $a_0(980)$ mass is shown in Fig. 2(c). The $\eta \pi^+ \pi^-$ mass spectrum for events with both $M(\eta \pi^+)$ and $M(\eta \pi^-)$ outside the $a_0(980)$ signal region is shown in Fig. 2(d). Comparison between Figs. 2(c) and 2(d) indicates that the $f_1(1285)$, $\eta(1405)$, and $X(1870)$ all primarily decay via the $a_0(980)\pi$ channel.

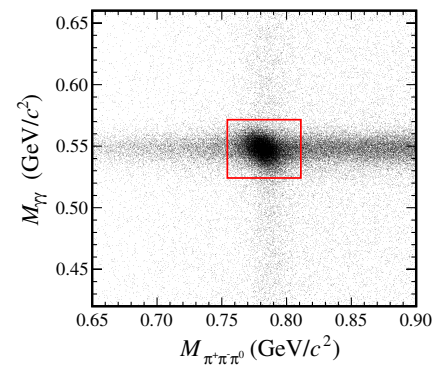


FIG. 1 (color online). Scatter plot of $M_{\eta(\gamma\gamma)}$ versus $M_{\omega(\pi^+ \pi^- \pi^0)}$. The rectangle in the middle shows the signal region defined as $|M_{\pi^+ \pi^- \pi^0} - m_\omega| < 28$ MeV/ c^2 and $|M_{\gamma\gamma} - m_\eta| < 24$ MeV/ c^2 .

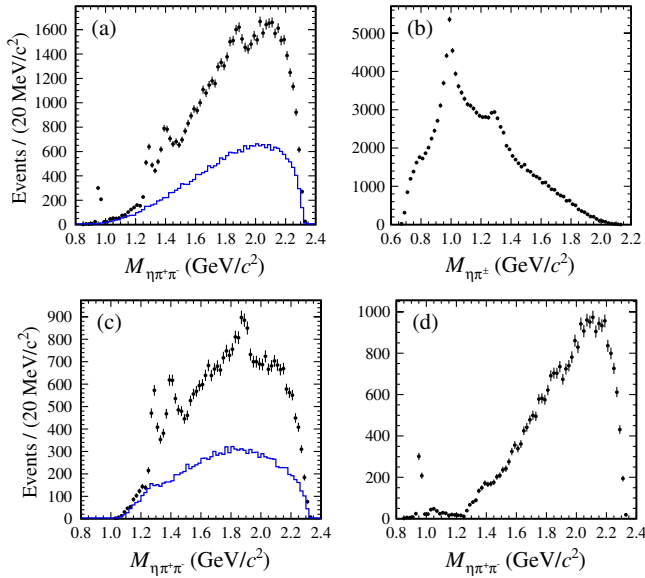


FIG. 2 (color online). Invariant-mass distributions for the selected events: (a) and (b) are the invariant-mass spectra of $\eta\pi^+\pi^-$ and $\eta\pi^\pm$ after the application of all the event-selection criteria; (c) is the $\eta\pi^+\pi^-$ mass spectrum for events with an $a_0(980)$ in the $\eta\pi^\pm$ final state; (d) is the $\eta\pi^+\pi^-$ invariant-mass distribution for events with no $a_0(980)$ in the $\eta\pi^\pm$ system. The histograms in (a) and (c) are the phase-space MC events of $J/\psi \rightarrow \omega\eta\pi^+\pi^-$ after the same event selection and with arbitrary normalization.

To ensure that the observed $f_1(1285)$, $\eta(1405)$ and the structure around $1.87 \text{ GeV}/c^2$ originate from the process of $J/\psi \rightarrow \omega a_0^\pm(980)\pi^\mp$ rather than peaking backgrounds, potential background channels are studied using both data and MC samples. The non- ω and/or non- $a_0(980)$ processes are estimated by the weighted sums of horizontal and vertical side bands, with the entries in the diagonal side bands subtracted to compensate for the double counting of background components. The definitions of the two-dimensional side bands are illustrated in Fig. 3. The weighting factors for the events in the horizontal, vertical, and the diagonal side bands are measured to be 0.48, 1.58,

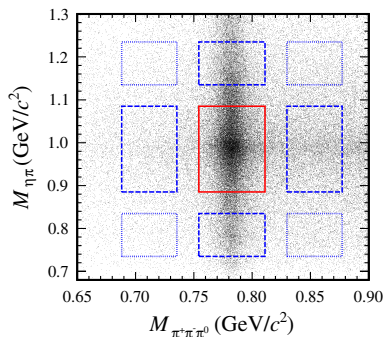


FIG. 3 (color online). Definition of the signal and two-dimensional side bands.

and 0.76, respectively, which are determined from the results of a two-dimensional fit to the mass spectrum of $M_\omega(\pi^+\pi^-\pi^0)$ versus $M_{a_0(980)}(\eta\pi)$. Here the two-dimensional probability density functions (PDFs) for $J/\psi \rightarrow \omega a_0(980)\pi$, ω but non- $a_0(980)$, non- ω but $a_0(980)$, non- ω and non- $a_0(980)$ processes are constructed by the product of one-dimensional functions, where the resonant peaks are parametrized by Breit-Wigner functions and the nonresonant parts are described by floating polynomials. To account for the difference of the background shape between the signal region and side bands due to the varying phase space, the obtained background $\eta\pi^+\pi^-$ mass distribution is multiplied by a correction curve determined from an MC sample of 2×10^6 events of the phase-space process $J/\psi \rightarrow \pi^+\pi^-\pi^0\eta\pi^+\pi^-$.

The background channel $J/\psi \rightarrow b_1(1235)a_0(980)$, where the $b_1(1235)$ decays to $\omega\pi$ and $a_0(980)$ decays to $\eta\pi$, is studied by performing a two-dimensional fit to the $M(\omega\pi)$ versus $M(\eta\pi)$ mass distribution with two-dimensional PDFs defined in similar fashion. We also studied an inclusive MC sample of 2×10^8 J/ψ decays generated according to the Particle Data Group (PDG) decay table and Lund-charm model [22]. No background-induced peaks are observed around $1.87 \text{ GeV}/c^2$. The inclusive MC sample is also used for the validation of the background estimation method described above, which is able to well reproduce the input background components.

Figure 4 shows the results of a fit to the $\eta\pi^+\pi^-$ mass spectrum where either $\eta\pi^+$ or $\eta\pi^-$ are in the $a_0(980)$ mass window. Here the three signal peaks are parametrized by Breit-Wigner functions convolved with a Gaussian resolution function and multiplied by an efficiency curve, which are both determined from signal MC samples and fixed in the fit. The background consists of three

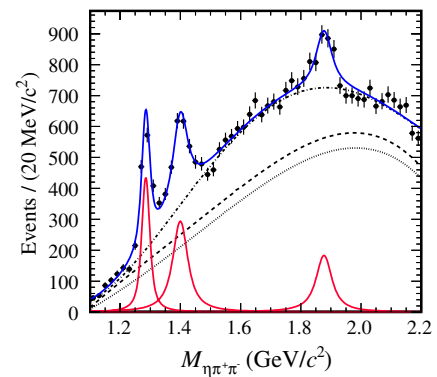


FIG. 4 (color online). Results of the fit to the $M(\eta\pi^+\pi^-)$ mass distribution for events with either the $\eta\pi^+$ or $\eta\pi^-$ in the $a_0(980)$ mass window. The dotted curve shows the contribution of non- ω and/or non- $a_0(980)$ background, the dashed line also includes the contribution from $J/\psi \rightarrow b_1(1235)a_0(980)$, and the dot-dashed curve indicates the total background with the non-resonant $J/\psi \rightarrow \omega a_0^\pm(980)\pi^\mp$ included. $\chi^2/\text{d.o.f.}$ is 1.27 for this fit.

components, namely, contributions from non- ω and/or non- $a_0(980)$ processes, $J/\psi \rightarrow b_1(1235)a_0(980)$ events, and nonresonant $\omega a_0(980)\pi$ processes. The background shapes and numbers of events for the non- ω and/or non- $a_0(980)$ processes are determined from the events in the two-dimensional side bands as discussed above, and fixed in the fit. For the $J/\psi \rightarrow b_1(1235)a_0(980)$ component of background, the background shape is fixed to that of the phase-space MC samples whereas the number of events is extracted and fixed to the result of a two-dimensional fit to the $\omega\pi$ versus $\eta\pi$ mass distributions. The contribution of the remaining nonresonant $\omega a_0(980)\pi$ process is described by a smooth floating polynomial function. The mass, width, and the product branching fractions obtained from the fit are summarized in Table I. For the $f_1(1285)$ and $\eta(1405)$, the measured mass and width are in agreement with PDG values [23]. The statistical significance of the $X(1870)$ signal is determined by the change of the log likelihood value and the degree of freedom in the fits with and without the assumption of an $X(1870)$. With all factors in the fit varied, the smallest change in the $-2\ln\mathcal{L}$ is 60.1, corresponding to a significance of 7.2σ . The same procedure is applied to the $f_1(1285)$ and $\eta(1405)$ signals, and the significances are determined to be much higher than 10σ .

The systematic errors on the measurement of the mass and width parameters are primarily due to the uncertainty in the fitting of the mass spectrum. In detail, the fit range, background estimation method, number of background events, and the background parametrization are varied to decide the uncertainty from the background estimation and fitting as a whole. We also include the systematic errors determined from the input-output checks based on the analysis of fully reconstructed MC samples, in which the input parameters are set according to the final results and the background is represented by the background channels seen in the inclusive MC sample. For systematic errors originating from the potential structure around $2.2\text{ GeV}/c^2$ and the multiple-event candidate selection, we refit the mass spectrum of $\eta\pi^+\pi^-$ with the inclusion of an $X(2120)$ resonance as recently reported by BESIII [2] in the decay channel of $J/\psi \rightarrow \gamma\eta'\pi^+\pi^-$, and all the valid multiple-entry candidates kept in order to estimate the

TABLE I. Summary of measurements of the mass, width, and the product branching fraction of $\mathcal{B}(J/\psi \rightarrow \omega X) \times \mathcal{B}(X \rightarrow a_0^\pm(980)\pi^\mp) \times \mathcal{B}(a_0^\pm(980) \rightarrow \eta\pi^\pm)$ where X represents $f_1(1285)$, $\eta(1405)$ and $X(1870)$. Here the first errors are statistical and the second ones are systematic.

Resonance	Mass (MeV/ c^2)	Width (MeV/ c^2)	$\mathcal{B}(10^{-4})$
$f_1(1285)$	$1285.1 \pm 1.0^{+1.6}_{-0.3}$	$22.0 \pm 3.1^{+2.0}_{-1.5}$	$1.25 \pm 0.10^{+0.19}_{-0.20}$
$\eta(1405)$	$1399.8 \pm 2.2^{+2.8}_{-0.1}$	$52.8 \pm 7.6^{+0.1}_{-7.6}$	$1.89 \pm 0.21^{+0.21}_{-0.23}$
$X(1870)$	$1877.3 \pm 6.3^{+3.4}_{-7.4}$	$57 \pm 12^{+19}_{-4}$	$1.50 \pm 0.26^{+0.72}_{-0.36}$

uncertainty due to these two sources, respectively. With the numbers from all the sources above combined quadratically, the systematic errors on the mass and width parameters are determined as shown in Table I.

The systematic errors on the branching fraction measurements are also subject to errors of the number of J/ψ events [17], the intermediate branching fractions [23], the data-MC difference in the π tracking efficiency, the photon detection efficiency, the kinematic fit, the signal-selection efficiency of η/π^0 , the simulation of the line shape of $a_0(980)$ [24], and the angular distributions due to different possible spin-parity hypotheses. Combined in quadrature with the influence from the mass spectrum fitting, the systematic errors on the product branching fraction for the $f_1(1285)$, $\eta(1405)$ and $X(1870)$ are summarized in Table I.

In summary, we present a study of the $J/\psi \rightarrow \omega\eta\pi^+\pi^-$ decay channel and report the first observation of the process $J/\psi \rightarrow \omega X(1870)$ in which $X(1870)$ decays to $a_0^\pm(980)\pi^\mp$, with the signal significance estimated to be 7.2σ . In the lower mass region of $\eta\pi^+\pi^-$ mass spectrum, the $f_1(1285)$ and $\eta(1405)$ are also clearly observed with statistical significances much larger than 10σ . The measurements of the mass, width, and product branching fraction of $\mathcal{B}(J/\psi \rightarrow \omega X) \times \mathcal{B}(X \rightarrow a_0^\pm(980)\pi^\mp) \times \mathcal{B}(a_0^\pm(980) \rightarrow \eta\pi^\pm)$ for the three resonant structures are summarized in Table I, wherein the product branching fractions for the $f_1(1285)$ and $\eta(1405)$ are measured for the first time. Whether the resonant structure of $X(1870)$ is due to the $X(1835)$, the $\eta_2(1870)$, an interference of both, or a new resonance still needs further study such as a partial wave analysis that will be possible with the larger J/ψ data sample that is anticipated in future runs of the BESIII experiment. For the $\eta(1405)$, the product branching fraction for its production in the hadronic decay of J/ψ is measured to be smaller than that for its production in the radiative J/ψ decays [23].

We thank the accelerator group and computer staff of IHEP for their effort in producing beams and processing data. We are grateful for support from our institutes and universities and from these agencies: Ministry of Science and Technology of China, National Natural Science Foundation of China, Chinese Academy of Sciences, Istituto Nazionale di Fisica Nucleare, Russian Foundation for Basic Research, Russian Academy of Science (Siberian branch), U.S. Department of Energy, and National Research Foundation of Korea.

- [1] M. Ablikim *et al.* (BES Collaboration), *Phys. Rev. Lett.* **95**, 262001 (2005).
- [2] M. Ablikim *et al.* (BESIII Collaboration), *Phys. Rev. Lett.* **106**, 072002 (2011).
- [3] S. L. Zhu and C. S. Gao, *Commun. Theor. Phys.* **46**, 291 (2006).

- [4] G.J. Ding and M.L. Yan, *Phys. Rev. C* **72**, 015208 (2005).
- [5] J.P. Dedonder *et al.*, *Phys. Rev. C* **80**, 045207 (2009).
- [6] J.Z. Bai *et al.* (BES Collaboration), *Phys. Rev. Lett.* **91**, 022001 (2003).
- [7] M. Ablikim *et al.* (BESIII Collaboration), *Chinese Phys. C* **34**, 421 (2010); J.P. Alexander *et al.* (CLEO Collaboration), *Phys. Rev. D* **82**, 092002 (2010).
- [8] T. Huang and S.L. Zhu, *Phys. Rev. D* **73**, 014023 (2006).
- [9] G. Hao, C.F. Qiao, and A.L. Zhang, *Phys. Lett. B* **642**, 53 (2006).
- [10] B.A. Li, *Phys. Rev. D* **74**, 034019 (2006).
- [11] N. Kochelev and D.P. Min, *Phys. Lett. B* **633**, 283 (2006).
- [12] D.L. Scharre *et al.*, *Phys. Lett. B* **97**, 329 (1980).
- [13] C. Edwards *et al.*, *Phys. Rev. Lett.* **49**, 259 (1982)..
- [14] T. Bolton *et al.* (Mark III Collaboration), *Phys. Rev. Lett.* **69**, 1328 (1992).
- [15] M. Acciarri *et al.* (L3 Collaboration), *Phys. Lett. B* **501**, 1 (2001).
- [16] L. Köpke and N. Wermes, *Phys. Rep.* **174**, 67 (1989).
- [17] M. Ablikim *et al.* (BESIII Collaboration), *Phys. Rev. D* **83**, 012003 (2011).
- [18] M. Ablikim *et al.* (BESIII Collaboration), *Nucl. Instrum. Methods Phys. Res., Sect. A* **614**, 345 (2010).
- [19] J.Z. Bai *et al.* (BES Collaboration), *Nucl. Instrum. Methods Phys. Res., Sect. A* **344**, 319 (1994).
- [20] S. Agostinelli *et al.* (GEANT4 Collaboration), *Nucl. Instrum. Methods Phys. Res., Sect. A* **506**, 250 (2003).
- [21] J. Allison *et al.*, *IEEE Trans. Nucl. Sci.* **53**, 270 (2006).
- [22] R.G. Ping, *Chinese Phys. C* **32**, 243 (2008).
- [23] K. Nakamura *et al.* (Particle Data Group), *J. Phys. G* **37**, 075021 (2010).
- [24] Jia-Jun Wu and B.S. Zou, *Phys. Rev. D* **78**, 074017 (2008).